

Structural, thermodynamic, and kinetic aspects of disordering in the pseudobrookite-type compound karröite, MgTi_2O_5

NANCY E. BROWN, ALEXANDRA NAVROTSKY

Department of Geological and Geophysical Sciences, Princeton University, Princeton, New Jersey 08544, U.S.A.

ABSTRACT

The pseudobrookite-type compound karröite (MgTi_2O_5) has been studied to understand how cation disordering, coupled with tight constraints of symmetry, affects its structural and thermodynamic properties and to address the kinetics of ordering. X-ray powder diffraction has been used to study the changes in lattice parameters of quenched samples at room temperature and in situ at temperatures between 973 and 1473 K. Enthalpies of annealing have been measured, using transposed-temperature-drop calorimetry, on two sets of quenched samples having different degrees of disorder. An empirical model that determines the degree of cation disorder from the c lattice parameter, along with the enthalpy data, has allowed assessment of various thermodynamic models of disordering. The data suggest the need to incorporate a term representing changes in the vibrational heat capacity with increasing disorder. The sigmoidal change in lattice parameters with increasing quench temperature results from slow ordering at $T < 973$ K and from unquenchable cation distributions (i.e., extremely rapid ordering) at $T > 1273$ K. The activation energy of ordering at $T < 973$ K is 212 ± 10 kJ/mol.

INTRODUCTION

Pseudobrookite-type compounds in the solid-solution series FeTi_2O_5 (ferropseudobrookite)– MgTi_2O_5 (karröite) received much attention during the Apollo missions because of their implications for the cooling histories of lunar basalts (Lind and Housley, 1972; Smyth, 1974; Wechsler et al., 1976). Members of the solid-solution series MgTi_2O_5 – Fe_2TiO_5 (pseudobrookite) have also been found in the Mg-rich Karroo volcanics in southeastern Zimbabwe and South Africa (Cox and Hornung, 1966). Their presence in many volcanic and metamorphic rocks has been attributed to high-temperature oxidation-exsolution of Mg-bearing hematite-ilmenite and ulvöspinel-magnetite phases (Rumble, 1976; Haggerty, 1976a, 1976b). Thus, pseudobrookite-related phases may be important indicators of thermal and oxygen-fugacity histories of geologic systems.

Pseudobrookite-type compounds exhibit unusually large thermal-expansion anisotropy (Bayer, 1971), and certain compositions exhibit positive enthalpies of formation, suggesting that their presence as high-temperature phases is due to entropy stabilization (i.e., a positive entropy of formation) (Navrotsky, 1975). Previous studies indicate that both the structural changes (Wechsler and Navrotsky, 1984; Wechsler, 1977) and high-temperature stabilization (Navrotsky, 1975) may be attributed to cation disordering. To better understand the disordering of pseudobrookite-type compounds, structural, calorimetric, and kinetic studies have been completed on karröite, MgTi_2O_5 .

SAMPLE PREPARATION AND EXPERIMENTAL TECHNIQUES

Samples previously synthesized from oxide mixes (Wechsler and Navrotsky, 1984) were annealed at temperatures between 773 and 1773 K in ~ 200 -mg batches enclosed in Pt foil. For temperatures at which cation equilibration was expected to be slow ($T < 873$ K), samples were annealed in a muffle furnace. At temperatures above 873 K, annealing experiments were carried out in a Deltech vertical-tube furnace. The Pt-foil capsules were suspended on a Pt wire in the furnace; they were quenched by melting the Pt wire, causing the sample to fall into liquid N_2 .

Room-temperature diffraction patterns were obtained by using a Scintag PAD V X-ray powder diffractometer equipped with a solid-state detector and utilizing $\text{CuK}\alpha$ radiation. NaCl was used as an internal standard in each X-ray scan. Lattice parameters were refined using the least-squares procedure of Appleman and Evans (1973). Seventeen to twenty-five reflections were used in the refinements over the range $15^\circ < 2\theta < 85^\circ$.

Heat contents ($H_T - H_{298}$) were measured using transposed-temperature-drop calorimetry in a Setaram HT 1500 calorimeter. A more complete description of the calorimeter and procedures can be obtained from Gaune-Escard and Bros (1974) and Ziegler and Navrotsky (1986). Briefly, the calorimeter was suspended in an alumina tube that separated it from an encircling graphite heating element. This design allowed the heating element to be run under a flow of Ar while the calorimeter was maintained

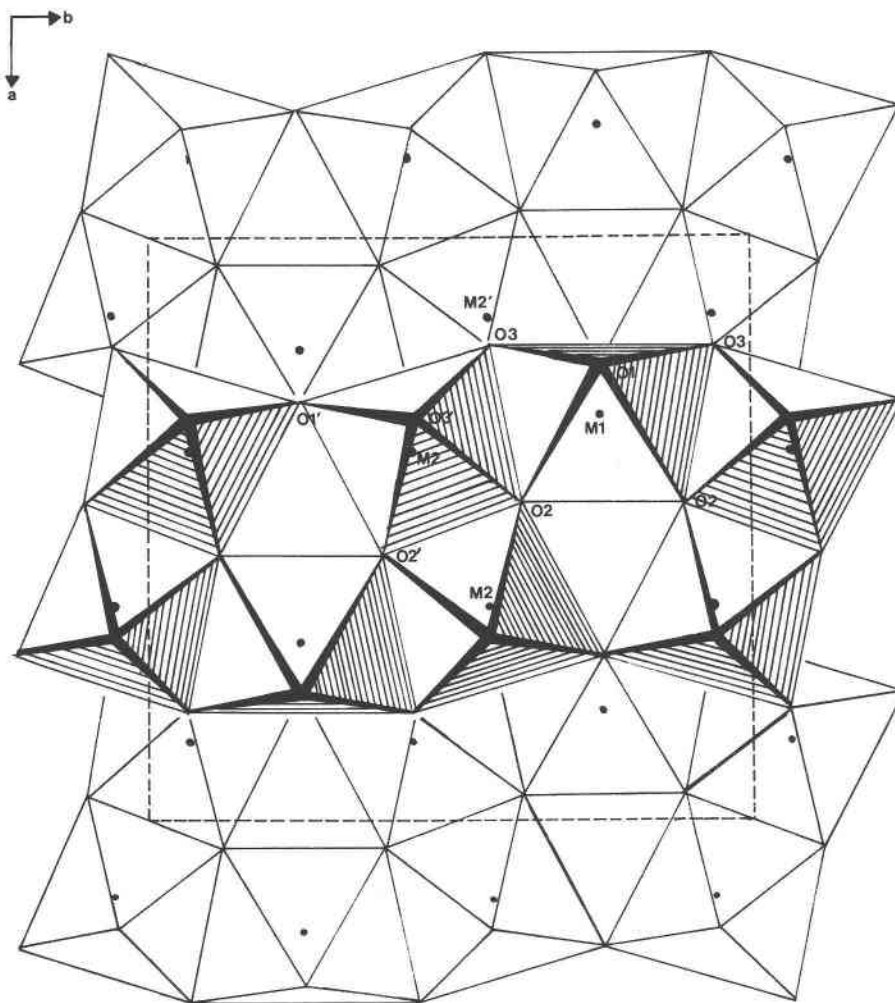


Fig. 1. The karrooite structure projected down the c axis. The a and b unit-cell parameters are shown by the dashed outline (modified from Wechsler et al., 1976).

in any desired gaseous atmosphere or in a vacuum. The experiments in this study were run at 10^{-3} bar to minimize convection. The calorimeter consisted of an upper thermopile surrounding a Pt-lined alumina crucible containing the MgTi_2O_5 sample and a lower reference thermopile surrounding a Pt-lined alumina crucible containing dried corundum powder. Following placement of the sample into the sample chamber and equilibration at room temperature, the sample was dropped into the calorimeter and its heat content measured.

Heat contents were measured on two sets of samples representing different initial states of disorder corresponding to quenching from 973 K and from 1273 K. In each case, we believe (see below) that the cation distribution characteristic of that temperature was retained in the quenched sample and that the cation distribution characteristic of the calorimeter temperature was attained rapidly during each calorimetric experiment. The 973-K samples were dropped into the calorimeter in the tem-

perature range 973–1773 K, whereas the 1273-K samples were studied at 1273–1773 K. Powdered samples weighing ~ 40 mg were placed in ~ 50 -mg Pt-foil capsules and compressed into as nearly spherical shapes as possible. This was done to ensure reproducible heat transfer between the sample and the Pt-lined alumina crucible. Ten karrooite drops were completed at each temperature. Corundum drops were alternated with each karrooite drop to determine daily calibration factors.

In situ high-temperature X-ray powder-diffraction data were obtained using a Scintag PAD v theta-theta diffractometer equipped with a heating stage (an Anton Paar unit, extremely modified in this laboratory) and scintillation detector ($\text{CuK}\alpha$ radiation). Temperatures to 1473 K were attained using a Pt resistance-strip heater, with an uncertainty in temperature of $\pm \sim 10$ K. Temperatures were measured using a Pt-Pt₈₇Rh₁₃ thermocouple and calibrated in a series of experiments using the thermal expansion of Pt and corundum and the melting point of

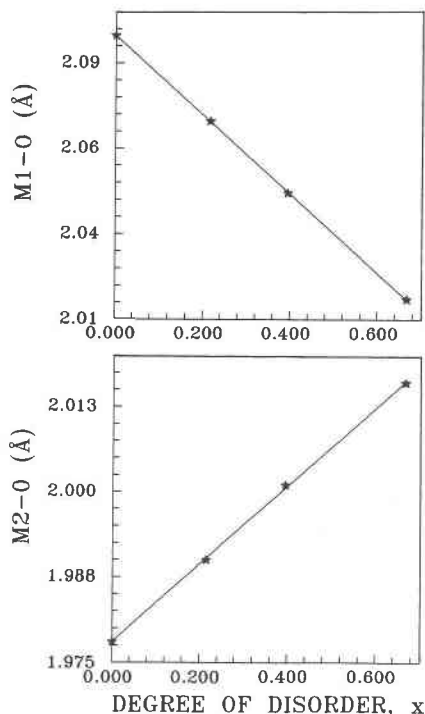


Fig. 2. Changes in the calculated (M1-O) and (M2-O) bond lengths plotted versus the degree of disorder in karrooite (see Table 1 for method of calculation).

NaCl. This made it possible to use the Pt sample holder as an internal standard, as well as to ensure proper alignment of the Pt-strip sample holder assembly. Resistances along the sample holder were closely controlled by modifying the shape of the Pt strip in order to limit thermal gradients across the 1-cm sample area to a maximum of 10 K at 1473 K.

STRUCTURAL BACKGROUND

Karrooite (MgTi_2O_5) has the pseudobrookite structure with a space group $Bbmm$ (Pauling, 1930). The structure

TABLE 1. Calculated mean (M1-O) and (M2-O) bond distances

	(M1-O) (Å)	(M2-O) (Å)	
Complete order (i.e., $x = 0$)			
100% Mg^{2+} in M1	2.093	100% Ti^{4+} in M2	1.978
$x = 0.217$			
78.3% Mg^{2+} in M1 21.7% Ti^{4+} in M1	2.068	10.85% Mg^{2+} in M2 89.15% Ti^{4+} in M2	1.990
$x = 0.395$			
60.5% Mg^{2+} in M1 39.5% Ti^{4+} in M1	2.047	19.75% Mg^{2+} in M2 80.25% Ti^{4+} in M2	2.001
Complete disorder (i.e., $x = 0.667$)			
33.3% Mg^{2+} in M1 66.7% Ti^{4+} in M1	2.016	33.35% Mg^{2+} in M2 66.65% Ti^{4+} in M2	2.016

Note: The mean oxygen radius has been calculated following the procedure of Wechsler (1977), where ${}^{16}\text{O}^{2-} = 0.72$, ${}^{18}\text{O}^{2-} = 1.36$, ${}^{16}\text{Ti}^{4+} = 0.605$, and ${}^{48}\text{O}^{2-} = 1.38$ Å and mean O^{2-} radius for M1 and M2 = $2(1.36) + 4(1.38) = 1.373$.

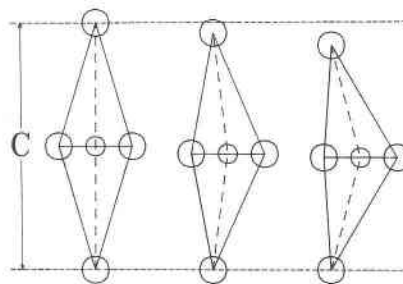


Fig. 3. Changes in the O-M-O octahedral bond angle caused by changes in site occupancy (Bayer, 1971). As the degree of disorder increases (from right to left), increasing Mg^{2+} enters the M2 site. This causes an increase on the O-M-O angle and a corresponding increase in the distance between the mirror planes at 0 and $\frac{1}{2}$ on the c axis (i.e., an increase in the height of the octahedra).

consists of distorted edge-sharing octahedra that form kinked bands parallel to the b axis (Fig. 1). All atoms in the unit cell lie on mirror planes at zero and $\frac{1}{2}$ on the c axis (Smyth, 1974). There are two crystallographically distinct octahedral sites, M1 and M2. The M1 site (Wyckoff notation 4c) has a site symmetry of mm and, in general, is larger and more distorted than M2. The M2 site (Wyckoff notation 8f) has a site symmetry of m (Wechsler, 1977; Smyth, 1974; Wechsler et al., 1976). Lind and Housley (1972) concluded after consideration of single-crystal X-ray data that in ordered MgTi_2O_5 , Mg^{2+} is preferentially incorporated into M1, whereas Ti^{4+} is preferentially incorporated into M2.

TABLE 2. Lattice parameters determined at room temperature and at high temperature

Quench T (K)	Room-temperature data					
	a (Å)*	a (Å)†	b (Å)*	b (Å)†	c (Å)*	c (Å)†
773	9.724(1)	9.731(2)	10.007(1)	10.004(2)	3.7392(4)	3.7400(7)
973	9.724(1)	9.728(2)	10.003(1)	10.003(1)	3.7412(4)	3.7416(4)
1098	9.734(1)	9.739(2)	9.994(1)	9.993(1)	3.7435(4)	3.7437(7)
1173	9.741(1)		9.990(1)		3.7452(5)	
1273	9.747(2)	9.745(2)	9.987(2)	9.986(2)	3.7456(7)	3.7459(2)
1373	9.748(1)	9.747(2)	9.984(1)	9.986(2)	3.7462(5)	3.7452(3)
1473	9.751(1)		9.984(1)		3.7464(4)	
1573	9.749(2)	9.749(1)	9.984(1)	9.984(1)	3.7458(6)	3.7455(6)
1673	9.750(1)	9.752(2)	9.981(1)	9.980(2)	3.7466(4)	3.7448(8)
1773	9.749(1)	9.748(2)	9.984(1)	9.982(1)	3.7463(5)	3.7450(15)
T (K)	High-temperature data					
	a (Å)†	b (Å)†	c (Å)†			
973	9.797(2)	10.098(2)	3.7508(8)			
1073	9.813(2)	10.111(2)	3.7530(5)			
1173	9.832(1)	10.122(1)	3.7554(7)			
1273	9.843(2)	10.133(1)	3.7572(4)			
1373	9.853(1)	10.150(2)	3.7592(7)			
1473	9.891(2)	10.179(2)	3.7619(7)			

Note: Number in parentheses indicates the standard deviation of the mean of the last digit.

* Data from Wechsler and Navrotsky (1984).

† Data from this study.

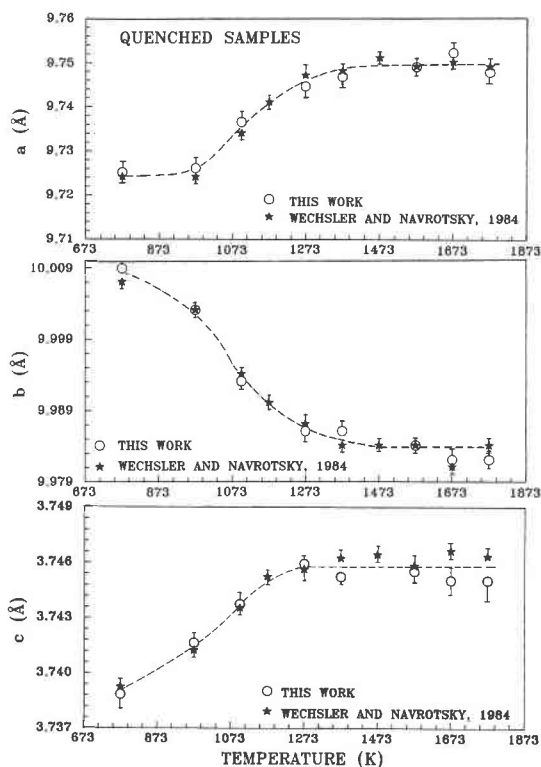


Fig. 4. Room-temperature lattice parameters as a function of quench temperature. Error bars represent the standard deviation of the mean. Dashed curves are visual fits to the data.

STRUCTURAL AND KINETIC STUDIES AT HIGH TEMPERATURE

Mean cation-oxygen bond lengths can be used to approximate structural changes arising from cation disorder. The $\langle M1-O \rangle$ and $\langle M2-O \rangle$ distances have been calculated for several cation distributions using the ionic radii of Shannon and Prewitt (1969) (Table 1). Complete order is described by having all Mg^{2+} in the M1 site and Ti^{4+} in the M2 site ($x = 0$ in Fig. 2), whereas complete disorder (a random distribution) is described by having $\frac{2}{3} Ti^{4+}$ and $\frac{1}{3} Mg^{2+}$ in M1 and $\frac{1}{3} Ti^{4+}$ and $\frac{2}{3} Mg^{2+}$ in M2 ($x = 0.667$ in Fig. 2). The overall decrease in size of the M1 site causes a net decrease in the b dimension because of a reduction in kinking of the octahedral chains (Fig. 1). Wechsler et al. (1976) ascribed this decrease in the b unit-cell parameter to octahedral edge sharing in the structure, with increasing disorder resulting in an overall decrease in the octahedral edge length due to increasing incorporation of Ti^{4+} (16% smaller than Mg^{2+}) into the M1 site. The net increase in size of the M2 site causes an increase in the a dimension (Fig. 1), whereas the very small increase in the c dimension is due to an increase in the mean O-M-O bond angle toward 180° (Bayer, 1971). This results in an increase in the height of the octahedra (Fig. 3). These relationships indicate an apparent dependence of b on the size of the M1 site, whereas a and c appear to depend on the size of M2.

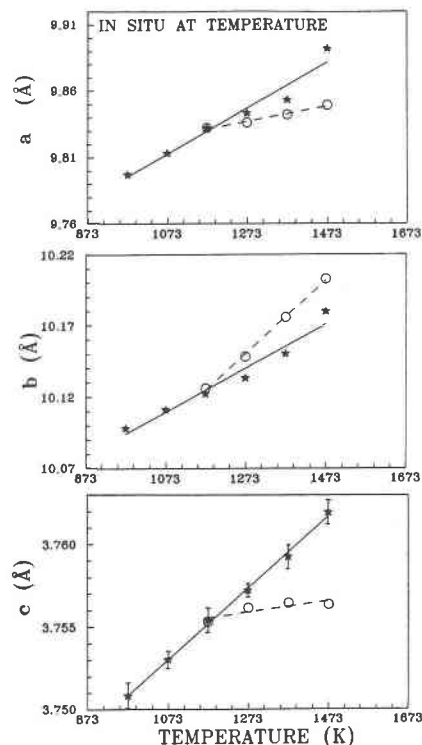


Fig. 5. High-temperature lattice parameters from in situ X-ray diffraction (filled stars). Solid lines represent linear best fits to the data. The open circles indicate the change in high-temperature lattice parameters expected if no further disordering occurred above 1273 K (see text), and the dashed lines are linear best fits to those points. Error bars represent the standard deviation of the mean where no error bars are shown.

The changes in lattice parameters of samples quenched from temperatures between 773 and 1773 K were determined using room-temperature X-ray powder-diffraction data (Fig. 4 and Table 2). These results agree well with those of Wechsler and Navrotsky (1984). When these measured changes are viewed in conjunction with calculated changes in the $\langle M1-O \rangle$ and $\langle M2-O \rangle$ bond lengths with increasing disorder (Fig. 2), it becomes evident that, as temperature increases, more Mg^{2+} occupies M2 while Ti^{4+} enters M1 (i.e., cation disorder increases). This was confirmed by earlier neutron-diffraction studies of several samples (Wechsler and Navrotsky, 1984). The sigmoidal shape of plots of the degree of disorder versus temperature can be interpreted in essentially two different ways: (1) there is no further disordering above ~ 1273 K, or (2) rapid order-disorder kinetics at temperatures greater than ~ 1273 K make these high-temperature cation distributions unquenchable.

These two possibilities can be distinguished using in situ high-temperature X-ray powder-diffraction (Fig. 5 and Table 2). Each sample was allowed to equilibrate at high temperature (973 to 1473 K) for 1 h to ensure an equilibrium cation distribution. The lattice parameters reflect

TABLE 3. Data on lattice parameters, site occupancy, and ionic radii for two armalcolite ($\text{Mg}_{0.5}\text{Fe}_{0.5}\text{Ti}_2\text{O}_5$) samples

673-K annealed sample		1373-K annealed sample	
Lattice parameters (Å)			
$a = 9.7454(5)$		$a = 9.7697$	
$b = 10.0625(4)$		$b = 10.0410$	
$c = 3.7422(1)$		$c = 3.7473$	
Site occupancy (mole fraction)			
M1	$\left\{ \begin{array}{l} \text{Fe} = 0.456 \\ \text{Mg} = 0.456 \\ \text{Ti} = 0.088 \\ \text{Fe} = 0.022 \end{array} \right.$	M1	$\left\{ \begin{array}{l} \text{Fe} = 0.367 \\ \text{Mg} = 0.367 \\ \text{Ti} = 0.266 \\ \text{Fe} = 0.066 \end{array} \right.$
M2	$\left\{ \begin{array}{l} \text{Mg} = 0.022 \\ \text{Ti} = 0.956 \end{array} \right.$	M2	$\left\{ \begin{array}{l} \text{Mg} = 0.066 \\ \text{Ti} = 0.867 \end{array} \right.$
Ionic radii, r (Å)			
$r_{\text{Mg}^{2+}} = 0.72$			
$r_{\text{Fe}^{2+}} = 0.77$			
$r_{\text{Ti}^{4+}} = 0.605$			

both the changes in cation distribution and the thermal expansion of each individual polyhedron. If no further disordering occurred above 1273 K, one would expect a change in slope in the high-temperature lattice-parameter data that parallels the change in slope of the room-temperature lattice-parameter data at $T > 1273$ K (Fig. 4).

It is possible to calculate the expansion of each lattice parameter arising solely from thermal effects, where for the a lattice parameter

$$\alpha_{a,\text{thermal}} = 1/a_{\text{quench}}[(a_{\text{in situ}} - a_{\text{quench}})/(T_{\text{in situ}} - 298)]. \quad (1)$$

In this equation $\alpha_{a,\text{thermal}}$ is the expansivity of the a lattice parameter due to purely thermal effects, a_{quench} is the room-temperature lattice parameter of a sample quenched from temperatures < 1273 K, $a_{\text{in situ}}$ is the in situ high-temperature lattice parameter, and $T_{\text{in situ}}$ is the temperature at which the lattice parameter was determined. Equation 1 was used to calculate $\alpha_{a,\text{thermal}}$ for samples quenched from temperatures from which the disordered state is quenchable ($T < 1273$ K). These results were used to extrapolate $\alpha_{a,\text{thermal}}$ above 1273 K. It was then possible to calculate what the hypothetical in situ a lattice parameter, $a'_{\text{in situ}}$, would be if the contribution from cation disordering was eliminated:

$$a'_{\text{in situ}} = a_{\text{quench},T}[1 + \alpha_{a,\text{thermal}}(T - 298)]. \quad (2)$$

The dashed lines in Figure 5 represent the hypothetical high-temperature lattice parameters of samples in which no further disordering occurs above 1273 K. In each case, the experimental data imply continued cation disordering above 1273 K. Therefore, the hypothesis of unquenchable cation distributions seems to be borne out. This is supported by the work of Wechsler and Navrotsky (1984) in which a maximum in the changes in lattice parameters, and thus a maximum in disordering for a particular temperature, occurred in weeks at 773 K, days at 873 K, an hour or less at 973 K, and presumably faster at higher temperatures.

DETERMINATION OF THE DEGREE OF DISORDER USING LATTICE PARAMETERS

An empirical model has been developed to determine the degree of disorder, x , from experimentally measured lattice parameters. This model views the systematic variation of oxygen positions, W , as being a function of (1) the sum of the mean cation radii of the M1 and M2 sites, $r = r_{\text{M1}} + r_{\text{M2}}$, and (2) the degree of disorder, x , where x is the mole fraction of Ti^{4+} on the M1 site. The armalcolite composition ($\text{Mg}_{0.5}\text{Fe}_{0.5}\text{Ti}_2\text{O}_5$) was chosen as a reference point to take advantage of excellent single-crystal X-ray data on samples with varying cation distributions (Wechsler, 1977; Smyth, 1974). Corresponding data are not available for MgTi_2O_5 . The variables r and x can be considered independent because the change in the mole fraction of three cations on two sites in armalcolite adds an additional degree of freedom.

Single-crystal X-ray diffraction data (Wechsler, 1977) on two armalcolite samples having different cation distributions (Table 3) have been used to determine linear relationships for $W(x)$ and $W(r)$. Following the method of Lager (1978), the initial oxygen positions in armalcolite can be expressed in vector components as

$$W_1 = w_1\mathbf{i} + w_2\mathbf{j} + w_3\mathbf{k}, \quad (3)$$

where w_1 , w_2 , and w_3 are the coordinates of a given oxygen atom in the unit cell. As r and x change, the position of a given coordinating oxygen moves to a final position:

$$W_2 = w_1\mathbf{i} + w_2\mathbf{j} + w_3\mathbf{k}. \quad (4)$$

For all calculations in this model, the initial reference state has been chosen as the armalcolite sample annealed at 673 K, and the final state is that annealed at 1373 K (Table 3).

The total change in oxygen position, dW , is given by the total differential

$$dW_{i,j,k} = (\partial W_{i,j,k}/\partial r_{\text{arm}})dr_{\text{comp}} + (\partial W_{i,j,k}/\partial x_{\text{arm}})dx. \quad (5)$$

In Equation 5, $(\partial W_{i,j,k}/\partial r_{\text{arm}})$ is the slope of a line representing the change in oxygen position accompanying a change in r_{arm} from the initial to the final state, where r_{arm} is calculated as

$$r_{\text{arm}} = [(X_{\text{Mg}} \cdot r_{\text{Mg}} + X_{\text{Fe}} \cdot r_{\text{Fe}} + X_{\text{Ti}} \cdot r_{\text{Ti}})_{\text{M1}} + (X_{\text{Mg}} \cdot r_{\text{Mg}} + X_{\text{Fe}} \cdot r_{\text{Fe}} + X_{\text{Ti}} \cdot r_{\text{Ti}})_{\text{M2}}]. \quad (6)$$

X_{Mg} , X_{Fe} , and X_{Ti} represent the mole fraction of Mg, Fe, and Ti in the M1 and M2 sites, and r_{Mg} , r_{Fe} , and r_{Ti} are the Shannon and Prewitt (1969) ionic radii of Mg^{2+} , Fe^{2+} , and Ti^{4+} in 6-fold coordination, respectively (Table 3). However, a very important point to realize is that r_{arm} is a function of the mole fractions, X , of Fe, Mg, and Ti on the M1 and M2 sites, which in turn depend on the degree of disorder, x . The term ∂r_{arm} is then obtained by

$$r_{\text{arm}} = d[r_{\text{arm}}(X(x))]/dx = [dr_{\text{arm}}/dX] \cdot [dX/dx]. \quad (7)$$

The r_{comp} term expresses only the change in r due to compositional differences between armalcolite and kar-

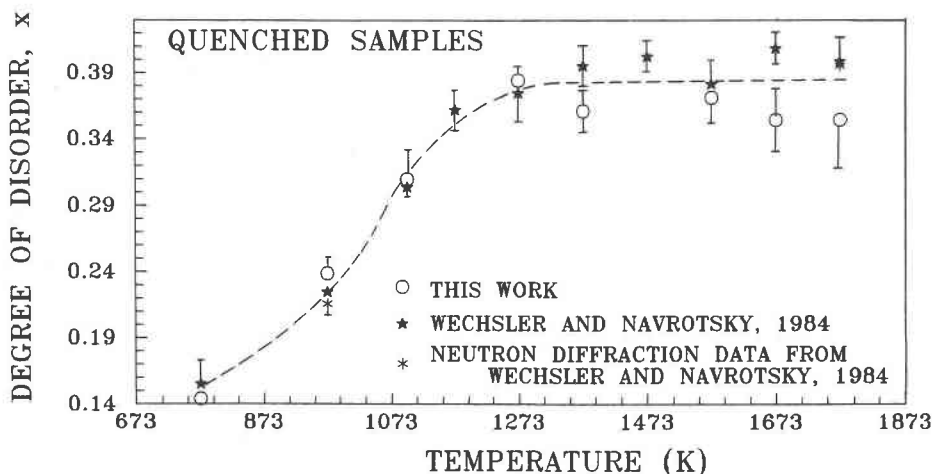


Fig. 6. Degrees of disorder calculated using the c lattice parameters determined on quenched samples in this study compared to those calculated from the lattice-parameter data of Wechsler and Navrotsky (1984). Degrees of disorder determined by neutron diffraction (Wechsler and Navrotsky, 1984) are also shown (note: the neutron-diffraction data point at 1773 K and $x = 0.395$ is somewhat obscured). Error bars have been calculated from the errors in the lattice-parameter data, and the dashed curve is a visual fit to the data.

roote. This is accounted for when the 2:1 ratio of M2: M1 sites is included in the calculation because r has a constant value for a specific composition. In this way, only the difference in r arising from the lack of Fe in karrooite will be expressed by the r_{comp} term. Thus, r_{comp} is calculated as

$$dr_{\text{comp}} = r_{\text{kar}} - r_{673,\text{arm}}, \quad (8)$$

where r_{kar} and $r_{673,\text{arm}}$ can be calculated from the generalized equation

$$r = \left(\sum_i X_i \cdot r_i / 2 \right)_{\text{M1}} + \left(\sum_i X_i \cdot r_i \right)_{\text{M2}}, \quad (9)$$

TABLE 4. Degree of disorder determined from c lattice parameters

Quench temperature (K)	c (Å)	x^*	x^\dagger	x^\ddagger
773	3.7392(4)	0.145(20)	0.155(14)	
973	3.7412(4)	0.238(14)	0.224(14)	
1098	3.7435(4)	0.309(24)	0.303(4)	
1173	3.7452(5)		0.361(17)	
1273	3.7456(7)	0.384(9)	0.374(24)	
1373	3.7462(5)	0.361(11)	0.395(17)	
1473	3.7464(4)		0.402(13)	
1573	3.7458(6)	0.371(20)	0.381(20)	
1673	3.7466(4)	0.347(26)	0.408(13)	
1773	3.7463(5)	0.354(50)	0.395(17)	0.316(5)

Note: Number in parentheses is the standard deviation of the mean in the last decimal place.

* Degree of disorder calculated from lattice parameters determined in this study.

† Degree of disorder calculated from lattice parameters of Wechsler and Navrotsky (1984).

‡ Degree of disorder determined by using single-crystal X-ray diffraction (Lind and Housley, 1972).

where X_i is the mole fraction and r_i is the ionic radii of the i th atom in the M1 and M2 sites.

The final term in Equation 5 is related to the degree of disorder, x , where $(\partial W_{i,j,k} / \partial x_{\text{arm}})$ is the slope of a line representing the change in oxygen position arising from the change in the degree of disorder from the initial to final state, and dx is the change in x between some unknown degree of disorder in karrooite and the degree of disorder in the initial reference state of armalcolite.

By selecting appropriate oxygen positions in the unit cell, it is possible to calculate the lattice parameters expected for a given degree of disorder. It is easiest to choose equivalent coordinating oxygen atoms in adjacent cells when calculating a and b . For c , any oxygen at $1/2$ on c will suffice, because symmetry constraints allow the c lattice parameter to be calculated directly (see below). The lattice parameters calculated from selected oxygen positions in karrooite with a measured degree of disorder of $x = 0.217$ (Wechsler and Navrotsky, 1984) are $a = 9.7388$

TABLE 5. Low-temperature annealing experiments

T (K)	Time (days)	c (Å)	x
723	58.3	3.7408(6)	0.210
723	77.5	3.7409(7)	0.214
773	20.8	3.7392(4)	0.155
773	50.1	3.7380(6)	0.114
823	34.2	3.7374(5)	0.094
823	49.3	3.7362(4)	0.053
823	71.3	3.7354(9)	0.025
873	0.05	3.7412(3)	0.224
873	0.2	3.7409(2)	0.214
923	0.03	3.7393(5)	0.176
923	0.08	3.7398(5)	0.159

Note: Number in parentheses represents the standard deviation of the mean in the last decimal place.

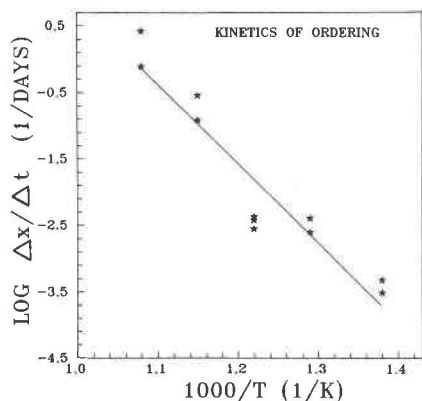


Fig. 7. Arrhenius plot of the \log_{10} rate of change in the c lattice parameter versus $1/T$ (K^{-1}). The solid line represents the best fit to all data points.

\AA , $b = 10.0683 \text{ \AA}$, and $c = 3.7408 \text{ \AA}$. Comparison with the measured values ($a = 9.724 \text{ \AA}$, $b = 10.003 \text{ \AA}$, and $c = 3.7412 \text{ \AA}$) determined by Wechsler and Navrotsky (1984) indicate that changes in the a and b lattice parameters are not predicted accurately by this model. This is probably because rotational distortions of the octahedra in the a - b plane in karrooite are not modeled well by using the changes in oxygen positions in armalcolite. However, the calculated value of c falls within the experimental uncertainty of the measurement. This probably arises from the constraint that coordinating oxygen atoms must lie on mirror planes at 0 and $1/2$ on the c axis. This constraint prevents rotation of the octahedra out of the a - b plane and, coupled with the large degree of edge sharing in the c direction, results in the high degree of sensitivity of the c lattice parameter to changes in cation distribution. Thus, even though c changes the least in magnitude with disorder, it is the most useful lattice parameter for calculating x .

The equation relating the total changes in oxygen positions to the the c unit-cell dimension is

$$c_{\text{kar}} = c_{673} + 2[(\partial W_k / \partial r_{\text{arm}}) dr_{\text{comp}} + (\partial W_k / \partial x_{\text{arm}}) dx], \quad (10)$$

where c_{673} is the c lattice parameter of the initial state of armalcolite and c_{kar} is the experimentally measured c lattice parameter of karrooite for which the degree of disorder is unknown. The factor of two arises from the choice of oxygen positions at $1/2$ on the c axis, and the remaining terms are those defined previously.

For $c = 3.7412 \text{ \AA}$ (a sample quenched from 973 K) and $c = 3.7463 \text{ \AA}$ (the average c for five samples quenched from temperatures above 1273 K), the calculated degrees of disorder are $x = 0.224$ and $x = 0.398$, respectively, in agreement with values determined by neutron diffraction, $x = 0.217$ and $x = 0.395$ (Wechsler and Navrotsky, 1984). The degrees of disorder calculated from lattice-parameter data of Wechsler and Navrotsky (1984) and this study are shown in Table 4 and Figure 6.

KINETIC STUDIES AT RELATIVELY LOW TEMPERATURES

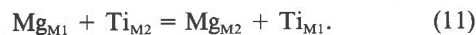
Below $\sim 873 \text{ K}$, the leveling off in lattice parameters of quenched samples can be attributed to slow rates of ordering. Annealing experiments were carried out at these temperatures to get a precise idea of the kinetics of the ordering process. The starting state of all powdered samples was the degree of disorder quenched from 973 K. These samples were annealed at temperatures between 723 and 923 K for intervals of 1 to ~ 80 d and the above technique was used to estimate the degree of disorder. Values of the rate of ordering, dx/dt , appear to vary at most by a factor of three (Table 5). However, owing to a lack of control over powder-particle size, it is unclear how much of this variation may arise from surface effects. Hence, a constant rate of ordering has been assumed.

An Arrhenius plot of $\log_{10}(dx/dt)$ versus $1/T$ (K^{-1}) (Fig. 7 and Table 5) provides values for the activation energy of the ordering process, $H_{\text{ord}} = 212 \pm 10 \text{ kJ/mol}$. This is similar to values from 214.2 to 360.9 kJ/mol obtained for various spinels (Grimes, 1972) and values of 208.4 kJ/mol for Mg-tracer diffusion in fayalite (Misener, 1974). Thus, kinetic processes involving M-site diffusion in a number of structures appear to have similar activation energies.

It may be possible to use the degree of ordering in pseudobrookite-type compounds as an indicator of the low-temperature thermal histories of lunar and terrestrial igneous rocks. However, studies of the ordering kinetics of Fe-bearing compositions would be needed.

CALORIMETRIC STUDIES

Disordering in the pseudobrookite structure is a non-convergent process involving two symmetrically distinct sites, M1 and M2, in a 1:2 ratio. Hence, this process is formally similar to disordering in spinels (Navrotsky and Kleppa, 1967) and can be written as



The configurational entropy, assuming random mixing of Ti and Mg on each set of sites, is

$$S_c = -R[x \ln x + (1-x) \ln(1-x) + x \ln(x/2) + (2-x) \ln(1-x/2)]. \quad (12)$$

Transposed-temperature-drop calorimetry can be used to study the enthalpies of disordering because the order-disorder process occurs quite rapidly above 973 K. The measured enthalpy consists of two contributions, that for heating the sample from room temperature to calorimeter temperature and that for changing the cation distribution (Fig. 8 and Table 6). For the sample quenched from 973 K and dropped to 973 K and that quenched from 1273 K and dropped to 1273 K, no change in the x occurs (see discussion of rates above) and the second enthalpy contribution is zero. Thus, these two samples define a line corresponding to the vibrational heat-capacity contribution with no change in x . One can extrapolate this line to

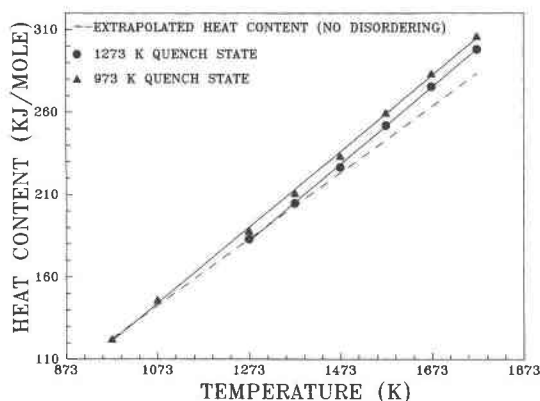


Fig. 8. Heat contents measured on samples having disordered states representative of 973 and 1273 K. The dashed line represents extrapolated heat contents of samples in which no disordering is involved. The size of the symbols represents two standard deviations of the mean.

higher temperatures (Fig. 8 and Table 6) to obtain the nonconfigurational heat-content contribution. This construction is supported by the Dulong-Petit limit

$$C_V = 3nR = 199 \text{ J/mol}\cdot\text{K}. \quad (13)$$

A value for C_p is then attained by adding the $C_p - C_V$ correction (i.e., $VT\alpha^2/\beta$), which amounts to a few percent. The value for C_p calculated from this line is 201 J/mol·K and is indeed slightly above the high-temperature Dulong-Petit limit, as expected. Deviations from this line can then be associated with enthalpy changes related to changes in x (Table 6 and Fig. 8). These deviations are termed enthalpies of annealing, ΔH_{anneal} , and are calculated by subtracting the extrapolated heat contents con-

TABLE 6. Heat contents measured by transposed-temperature-drop calorimetry

T (K)	Measured heat contents* ($H_T - 298$) (kJ/mol)	No disordering contribution (kJ/mol)	Enthalpy of annealing† ΔH_{anneal} (kJ/mol)
Samples quenched from 973 K			
973	122.5 ± 0.8 [10]	122.5 ± 0.8* [10]	
1073	148.1 ± 1.9 [8]	143.0 ± 2.1‡	5.1 ± 3.9
1273	190.8 ± 2.8 [10]	182.9 ± 2.8* [8]	7.9 ± 4.2
1473	233.7 ± 3.6 [9]	223.2 ± 3.3‡	10.5 ± 4.9
1573	259.8 ± 4.2 [8]	243.3 ± 3.6‡	16.5 ± 5.5
1673	283.6 ± 3.5 [9]	263.4 ± 3.9‡	20.2 ± 5.2
1773	306.3 ± 4.3 [8]	283.6 ± 4.3‡	22.7 ± 6.1
Samples quenched from 1273 K			
1273	182.9 ± 2.7 [8]	182.9 ± 2.8* [8]	
1473	226.7 ± 2.8 [8]	223.2 ± 3.3‡	3.5 ± 4.3
1573	259.8 ± 4.2 [8]	243.3 ± 3.6‡	8.9 ± 5.1
1673	283.6 ± 3.5 [9]	263.4 ± 3.9‡	12.3 ± 5.7
1773	306.3 ± 4.3 [8]	283.6 ± 4.3‡	14.7 ± 5.3

Note: The number in brackets represents the number of experiments included in the mean.

* Error represents two standard deviations of the mean.

† Errors are calculated as the square root of the sum of the squares.

‡ Errors have been estimated at 1.5% of the heat-content value.

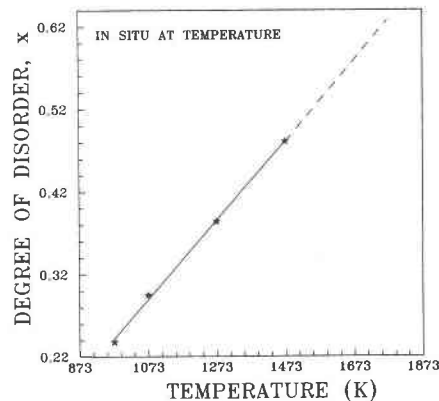


Fig. 9. Plot of x versus T , where x has been calculated from the in situ values of c determined by high-temperature X-ray powder diffraction and corrected for constant thermal expansivity.

taining no disordering contribution from measured heat contents for the two sets of samples.

In order to check whether observed values of ΔH_{anneal} contained any contribution from possible Ti reduction under the 10^{-3} bar vacuum conditions of the calorimeter, weight-loss experiments were completed in the temperature range 1373 to 1773 K, using a Deltech vertical-tube furnace under 10^{-3} bar vacuum conditions similar to those in the calorimeter. Samples were quenched to room temperature under vacuum conditions in order to avoid possible reoxidation that might occur using the standard quenching technique. Weight changes ranged from -0.02% to $+0.03\%$ and show that oxygen loss must be less than ~ 0.5 wt%. Thus, any substantial contributions to ΔH_{anneal} arising from Ti reduction are unlikely.

Interpretation of the enthalpy of annealing data requires knowledge of the degree of disorder at temperatures where cation distributions are unquenchable. Figure 9 shows a plot of x versus T , where x is calculated from the in situ values of c corrected for constant lattice expansivity (as discussed above). This plot is strikingly lin-

TABLE 7. Values of x_{cal} calculated from in situ high-temperature lattice-parameter data

T (K)	x_{cal}^*	x_{cal}^\dagger
973	0.238	0.224
1073	0.295	0.287
1273	0.384	0.374
1473	0.481	0.474
1573‡	0.530	0.524
1673‡	0.578	0.574
1773‡	0.627	0.624

* Degree of disorder calculated by using lattice-parameter data from this study.

† Degree of disorder calculated by using lattice-parameter data from Wechsler and Navrotsky (1984).

‡ Values of the degree of disorder at temperatures above 1473 K have been extrapolated from the low-temperature data.

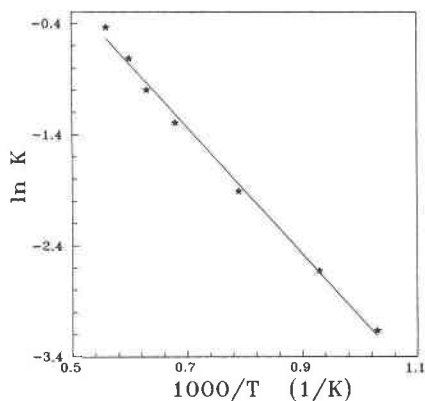


Fig. 10. Plot of $\ln K$ versus $1/T$, where $K = x^2/[(1-x)(2-x)]$ (Navrotsky and Kleppa, 1967). This chemical-equilibrium approach indicates that the nonconfigurational entropy is not zero.

ear (as opposed to sigmoidal for quenched samples) and is consistent with continued disordering with increasing temperature. Extrapolating this line to temperatures above 1473 K, the highest temperature of our X-ray measurements, provides estimates of x for calorimetric samples dropped to temperatures from 1473 to 1773 K (Table 7). This extrapolation predicts a value of $x = 0.70$ at the melting temperature (~ 1923 K). This value is close to (actually slightly greater than) the degree of disorder for random cation distribution ($x = 0.667$), which would correspond to a maximum configurational entropy.

Equipped with knowledge of the enthalpy of annealing and values for the degree of disorder at temperatures above 1273 K, it then becomes possible to evaluate the thermodynamics of disordering in MgTi_2O_5 . A number of formalisms have been proposed to describe the thermodynamics of disordering in spinels. These act as good starting points for evaluating the behavior of karrooite.

The simplest of these models (Navrotsky and Kleppa,

TABLE 8. Enthalpies of annealing, enthalpies of disordering, and free energies of disordering for different thermodynamic models

T (K)	Measured ΔH_{anneal} (kJ/mol)	Calculated			
		ΔH_{anneal} (kJ/mol) Navrotsky- Kleppa model	ΔG_{D} (kJ/mol) O'Neill-Navrotsky model	ΔH_{D} (kJ/mol)	ΔG_{D} (kJ/mol) C_{PD} model
973	0	0	25.6	43.7	23.0
1073	5.1*	2.7	23.4	47.8	21.7
1273	7.9*	6.9	20.2	54.3	18.7
1473	10.5*	11.5	15.0	61.3	15.0
1573	16.5*	13.8	11.8	64.9	13.0
1673	20.2*	16.1	8.1	68.3	10.9
1773	22.7*	18.4	3.9	71.9	8.6
1473	3.5†	4.6			
1573	8.9†	6.9			
1673	12.3†	9.2			
1773	14.7†	11.5			

* Experiments completed on samples quenched from 973 K.

† Experiments completed on samples quenched from 1273 K.

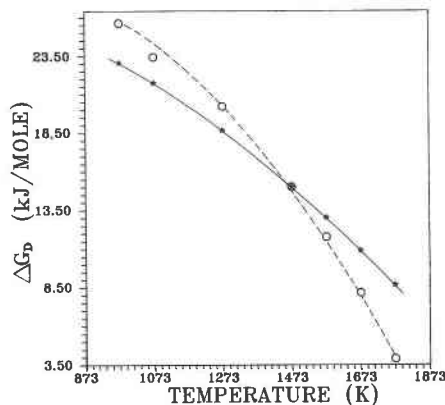


Fig. 11. Comparison of the $\Delta G_{\text{D},T}$ values obtained when calculated as $\Delta G_{\text{D},T} = -RT \ln\{x^2/[(1-x)(2-x)]\}$ (filled stars and solid line) and as $\Delta G_{\text{D},T} = \Delta H_{\text{D},T_0} + (\Delta C_p)_b(T - T_0) - T\{\Delta S_{\text{D},T_0} + (\Delta C_p)_b \ln(T/T_0)\}$ (open circles and dashed line).

1967) describes the mixture of Mg and Ti on each sublattice as ideal. The enthalpy of the interchange reaction (Eq. 11) has a constant value (i.e., is independent of the degree of disorder). One can consider Equation 11 as a chemical equilibrium for which the equilibrium constant is

$$K = (\text{Ti}_{\text{M1}})(\text{Mg}_{\text{M2}})/(\text{Mg}_{\text{M1}})(\text{Ti}_{\text{M2}}) = x^2/[(1-x)(2-x)] \quad (14)$$

and

$$\ln K = -\Delta G_{\text{D}}/RT = \Delta S_{\text{D}}/R - \Delta H_{\text{D}}/RT. \quad (15)$$

The nonconfigurational entropy of disordering, ΔS_{D} , is given by the intercept of a plot of $\ln K$ vs. $1/T$ and the enthalpy of disordering, ΔH_{D} , is given by the slope (Fig. 10). From the data in Table 8 and Figure 10, values for the enthalpy and nonconfigurational entropy of disordering are $\Delta H_{\text{D}} = 47.34$ kJ/mol and $\Delta S_{\text{D}} = 2.65$ J/mol·K, respectively. It is important to note that in many spinels, the nonconfigurational entropy of disordering is approximately zero (Navrotsky and Kleppa, 1967). However, this is not the case for karrooite (see below).

The enthalpy of annealing data can then be analyzed as

$$\Delta H_{\text{anneal}} = \Delta H_{\text{D}}(x_{\text{cal}} - x_{\text{quench}}), \quad (16)$$

where the terms x_{cal} and x_{quench} are the degree of disorder of samples in situ in the calorimeter and those of the quenched reference states, respectively. Comparison of calculated and measured values of ΔH_{anneal} (Table 8) shows that, in general, the measured values are underestimated by ~ 20 – 50% . Hence, a simple model where the energetics of cation disordering is independent of the degree of disorder is not adequate for MgTi_2O_5 .

Following the formalism of O'Neill and Navrotsky (1983), a more complicated approach can be taken where the enthalpy of disordering is dependent on the degree of disorder:

$$\Delta H_{\text{D}} = Ax + Bx^2. \quad (17)$$

The enthalpy of annealing data and the values of x determined above can be used to obtain values of A and B . The enthalpy of annealing is

$$\Delta H_{\text{anneal}} = A(x_{\text{cal}} - x_{\text{quench}}) + B(x_{\text{cal}}^2 - x_{\text{quench}}^2). \quad (18)$$

A least-squares fit to the data involving nine equations of the form of Equation 18 gives $A = 26.3888$ kJ/mol and $B = 36.2802$ kJ/mol. Statistically, the quality of the fit is acceptable.

If one compares values of ΔG_D obtained from values of x and calculated as

$$\Delta G_D = -RT \ln[x^2/(1-x)(2-x)] \quad (19)$$

with values of ΔH_D obtained from Equation 17, it becomes obvious that ΔS_D must vary in a complementary fashion to ΔH_D in order to account for the values of ΔG_D and preserve linearity in the plot of $\ln K$ vs. $1/T$ (Table 8 and Fig. 10). Since ΔG_D varies roughly linearly with T , while ΔH_D varies with x with both a linear and quadratic term (Eq. 17) and x varies virtually linearly with T (Fig. 9), this approach forces ΔS_D to depend on terms both linear and quadratic in x . This behavior, though not impossible, requires fitting the data with four seemingly independent parameters, namely A and B terms for both the enthalpy and entropy of disordering. Because of the virtually linear relation between x and T (Fig. 9) inferred from the variation of c with T , it is operationally impossible to distinguish whether a given thermodynamic parameter depends more simply on x or on T .

The above model assumes that the enthalpy and entropy of disordering depend on temperature only through their dependence on x . Thus, the differences in lattice vibrations that lead to ΔS_D are assumed to make their major contributions well below the temperature at which the structural and thermodynamic studies were done. However, the structural studies suggest a strong coupling between x and the unit-cell parameters at high and low temperature, as well as highly anisotropic thermal expansion at all temperatures.

Further evidence for possible changes in lattice vibrations can be seen in the increase in temperature factors, particularly for oxygen (Wechsler, 1977) with increasing cation disorder. These increases reflect differing local cation arrangements in the disordered material. Hence, relating the variations of the enthalpy and entropy of disorder to contributions from a change in vibrational heat capacity on disordering, $\Delta C_{P,D}$, may provide an appropriate avenue through which the increased structural distortions accompanying disordering in pseudobrookite-type compounds can be incorporated into a thermodynamic formalism. These ideas can be formalized in a third approach, which retains a simple linear dependence of ΔH_D and ΔS_D on x , but incorporates the effects of a significant $\Delta C_{P,D}$ term, associated with disordering, on both ΔH_D and ΔS_D . This approach describes the data more economically, and perhaps has more direct physical meaning, than the above four-parameter description. The free energy of disordering then becomes

$$\Delta G_D = \Delta H_{D,T_0} + \Delta C_{P,D}(T - T_0) - T[\Delta S_{D,T_0} + \Delta C_{P,D} \ln(T/T_0)]. \quad (20)$$

In these equations, T_0 is the quench temperature of the reference state (i.e., 973 or 1273 K) and T is the temperature at which the entropy, ΔS_D , and enthalpy, ΔH_D , of disordering is sought.

The enthalpy of annealing is fit using

$$\Delta H_{\text{anneal}} = A + B(T - T_0), \quad (21)$$

where $A = \Delta H_{D,T_0}$, $B = \Delta C_{P,D}$, and T is the temperature at which the enthalpy of annealing is determined (i.e., the calorimeter temperature). For enthalpies of annealing determined on samples quenched from 973 K, Equation 21 becomes

$$\Delta H_{\text{anneal}} = A(x_{\text{cal}} - x_{\text{quench}}) + Bx_{\text{cal}}(T - 973). \quad (22)$$

For the 1273-K quenched samples, the constant A is replaced by A' , where

$$A' = A + B(1273 - 973) = A + 300B. \quad (23)$$

The expression for the ΔH_{anneal} of samples with $x_{T=1273}$ becomes

$$\Delta H_{\text{anneal}} = A(x_{\text{cal}} - x_{\text{quench}}) + B[300(x_{\text{cal}} - x_{\text{quench}}) + x_{\text{cal}}(T - 1273)]. \quad (24)$$

Equations 22 and 24 were applied to the enthalpy of annealing data. Values of x_{cal} were substituted into these equations, and A and B were determined by a least-squares analysis of five equations of the form of Equation 22 and four equations of the form of Equation 24 to give $A = 34.8239$ kJ/mol and $B = 17.8$ J/mol·K. The fit to the data is as good as in the model above. These values of A and B can then be used to calculate $\Delta H_{D,T}$, $\Delta G_{D,T}$, and $\Delta S_{D,T}$. Agreement between $\Delta G_{D,T}$ values calculated using Equation 20 and those calculated from Equation 19 can be seen in Figure 11 and Table 8. Although the fit to the data is not perfect, it does describe the free-energy curve quite well. This indicates that a thermodynamic model including a $\Delta C_{P,D}$ term may be appropriate for describing cation disordering in pseudobrookite-type compounds. It would be interesting to see whether the vibrational spectra of MgTi_2O_3 are sensitive to the degree of disorder.

CONCLUSIONS

Consideration of both structural and thermodynamic data on karrooite provides a more complete understanding of the effects of cation disordering at the atomic scale. The changes in the a , b , and c lattice parameters with increasing disorder and the extreme sensitivity of the c parameter to small changes in x reflect the responses of the individual polyhedra to changes in cation occupancy. These responses are accentuated by the large degree of edge sharing in all directions and the constraints of symmetry that require all atoms to lie on special sites within the unit cell. With increasing disorder, the distortions of the individual polyhedra change, corresponding to the changes in bond length necessary to absorb the 16% dif-

ference in ionic radii between Mg and Ti. The overall result is to create more random local cation-anion arrangements, as indicated by the increase in temperature factors (Wechsler, 1977). The effect may give rise to the changes in vibrational heat capacity necessary to explain the free energies and enthalpies of disordering.

Data on the kinetics of ordering indicate that the degree of disorder in pseudobrookite-type compounds may provide information on thermal histories, particularly at low temperatures where the rate of ordering is on a geologic time scale.

ACKNOWLEDGMENTS

This research was supported by NSF grant DMR 8610816. We also gratefully acknowledge Dr. S. Swapp for her assistance with all aspects of X-ray diffraction. Charles Bennett and Charles Kulick helped redesign the PAAR HTK controller.

REFERENCES CITED

- Appleman, D.E., and Evans, H.T., Jr. (1973) Indexing and least squares refinement of powder diffraction data. U.S. Geological Survey Computer Contribution 20, 62 p.
- Bayer, G. (1971) Thermal expansion and stability of pseudobrookite-type compounds, Me_3O_5 . *Journal of Less Common Metals*, 24, 129–138.
- Cox, L.G., and Hornung, G. (1966) The petrology of the Karroo Basalts of Basutoland. *American Mineralogist*, 51, 1414–1432.
- Gaune-Escard, M., and Bros, J.P. (1974) High-temperature calorimetry up to 1800 K. *Canadian Metallurgical Society of Quebec*, 13, 335–338.
- Grimes, N.W. (1972) Self diffusion in compounds with spinel structure. *Philosophical Magazine*, 25, 67–76.
- Haggerty, S.E. (1976a) Oxidation of opaque mineral oxides in basalts. *Mineralogical Society of America Reviews in Mineralogy*, 3, Hg1–Hg100.
- (1976b) Opaque minerals in terrestrial igneous rocks. *Mineralogical Society of America Reviews in Mineralogy*, 3, Hg101–Hg300.
- Lager, G.A. (1978) A novel technique for characterizing thermal expansion in minerals. *Physics and Chemistry of Minerals*, 3, 237–249.
- Lind, M.D., and Housley, R.M. (1972) Crystallization studies of lunar igneous rocks: Crystal structure of synthetic armalcolite. *Science*, 175, 521–523.
- Misener, D.J. (1974) Cation diffusion in olivine to 1400 °C and 35 kbar. In H.S. Yoder, Jr., Ed., *Geochemical kinetics*, p. 117–129. Carnegie Institution of Washington, Washington, D.C.
- Navrotsky, A. (1975) Thermodynamics of formation of some compounds with the pseudobrookite structure and of the FeTi_2O_5 - Ti_3O_5 solid solution series. *American Mineralogist*, 60, 249–256.
- Navrotsky, A., and Kleppa, O.J. (1967) The thermodynamics of cation distributions in simple spinels. *Journal of Inorganic Nuclear Chemistry*, 30, 479–498.
- O'Neill, H.St.C., and Navrotsky, A. (1983) Simple spinels: Crystallographic parameters, cation radii, lattice energies, and cation distribution. *American Mineralogist*, 68, 181–194.
- Pauling, L. (1930) The crystal structure of pseudobrookite. *Zeitschrift für Kristallographie*, 73, 97–112.
- Rumble, D., III. (1976) Oxide minerals in metamorphic rocks. *Mineralogical Society of America Reviews in Mineralogy*, 3, R1–R24.
- Shannon, R.D., and Prewitt, C.T. (1969) Effective ionic radii in oxides and fluorides. *Acta Crystallographica*, B25, 925–946.
- Smyth, J.R. (1974) The crystal chemistry of armalcolite from Apollo 17. *Earth and Planetary Science Letters*, 24, 262–270.
- Wechsler, B.A. (1977) Cation distribution and high-temperature crystal chemistry of armalcolite. *American Mineralogist*, 62, 913–920.
- Wechsler, B.A., and Navrotsky, A. (1984) Thermodynamic and structural chemistry of compounds in the system MgO-TiO_2 . *Journal of Solid State Chemistry*, 55, 165–180.
- Wechsler, B.A., Prewitt, C.T., and Papike, J.J. (1976) Chemistry and structure of lunar and synthetic armalcolite. *Earth and Planetary Science Letters*, 29, 91–103.
- Ziegler, D., and Navrotsky, A. (1986) Direct measurement of the enthalpy of fusion of diopside. *Geochimica et Cosmochimica Acta*, 50, 2461–2466.

MANUSCRIPT RECEIVED OCTOBER 5, 1988

MANUSCRIPT ACCEPTED MARCH 9, 1989